文章编号：1001-9014(2021)05-0680-05

DOI:10.11972/j.issn.1001-9014.2021.05.015

Effective enhancement of the photoluminescence from the Si^+/Ni^+ ions co-implanted SOI by directly constructing the nanodisk photonic crystals

TONG Hao-Chen[1], TANG Shu-Min[1], YE Shu-Ming[1], Duan Xiao-xiao[1], LI Xiao-Nan[1], XIE Ji-Yang[1], ZHANG Lu-Ran[1], YANG Jie[1], QIU Feng[1], WANG Rong-Fei[1*], WEN Xiao-Ming[2], Yang Yu[1], CUI Hao-Yang[3], WANG Chong[1*]

(1. National Center for International Research on Photoelectric and Energy Materials, School of Materials and Energy, Yunnan University, Kunming 650091, China;
2. Centre for Translational Atomaterials, Swinburne University of Technology, Hawthorn 3122, Australia;
3. College of Electronic and Information Engineering, Shanghai University of Electric Power, Shanghai 200090, China.)

Abstract: An effective enhancement of the photoluminescence from the Si^+/Ni^+ ions co-implanted silicon-on-insulator (SOI) by directly constructing the Au nanodisk-array photonic crystals is reported. The finite-difference time-domain method (FDTD) was employed to design and analyze the luminescence amplification of the metal film with a photonic crystal structure for luminesce from the optical defects in the SOI. The Langmuir-Blodgett (LB) method and inductively coupled plasma (ICP) etching were used to fabricate the etched Au-nanostructure photonic crystal directly on the top of SOI wafers. It indicates that the introduction of polystyrene (PS) spheres can effectively improve the luminescent efficiency in the near infrared waveband. This photonic crystal with simply fabricating processes and high efficiency exhibits great application on the optical quantum of Si-based photonics.

Key words: infrared physics, photoluminescence, ion co-implantation, silicon on insulator, photonic crystal, plasma

纳米盘光子晶体增强 Si^+/Ni^+ 离子共注入 SOI 的光致发光

童浩辰[1], 唐淑敏[1], 叶书鸣[1], 段潇潇[1], 李晓南[1], 谢继阳[1], 张璐然[1], 杨 杰[1], 邱 峰[1], 王荣飞[1*], 文小明[2], 杨 宇[1], 崔昊杨[3], 王 茺[1*]

(1. 云南大学 材料与能源学院,国家光电子与能源材料国际研究中心,云南 昆明650091;
2. 斯威本科技大学 平动原子材料中心,霍桑 3122,澳大利亚;
3. 上海电力大学 电子与信息工程学院,上海 200090)

摘要:报道了一种在 Si^+/Ni^+ 离子共注入绝缘体上硅(SOI)基片上直接构筑纳米盘阵列光子晶体以实现SOI光致发光有效增强的方法。通过时域有限差分法(FDTD)设计出具有荧光增强效应的光子晶体结构金属膜,利用 Langmuir-Blodgett(LB)方法在 Si^+/Ni^+ 离子共注入SOI上排列一层聚苯乙烯(PS)小球,接着沉积一层Au薄膜,然后用电感耦合等离子体(ICP)蚀刻技术在SOI晶片顶部形成了纳米盘状的刻蚀Au光子晶体。光致发光(PL)实验表明光子晶体的引入有效增强了缺陷Si薄膜在近红外波段的发光效率。这种工艺简单、成本低且发光增益高的光子晶体在硅基集成光子学上具有重要的应用前景。

Received date: 2020-12-29, **revised date**: 2021-07-05　　**收稿日期**:2020-12-29,**修回日期**:2021-07-05

Foundation items: Supported by the National Natural Science Foundation of China (11564043, 11504322, 11704330), Joint Foundation of Provincial Science and Technology Department-Double First-class Construction of Yunnan University (2019FY003016), the Reserve Talents of Academic and Technical Leader Project (2017HB001), Young Top Talent Project(YNWR-QNBJ-2018-229), and the Application Basic Research Project (2019FB130) of Yunnan Province.

Biography: TONG Haochen (1997-), male, Zhejiang, China, Master student of Yunnan University. His current research interests include Photonic crystals, magnetic semiconductors and silicon-based spin semiconductors. E-mail: 2212301592@qq.com

* **Corresponding author**: E-mail: rfwang@ynu.edu.cn, cwang@ynu.edu.cn

关 键 词: 红外物理; 光致发光; 离子共注入; 绝缘体上硅; 光子晶体; 等离子体
中图分类号: O433.2 **文献标识码**: A

Introduction

Generally, the defect states in semiconductors can play a vital role in degrading its electrical and photoelectronic performance. Some deep-level defects can be introduced artificially into the indirect band gap semiconductors and then transformed to be optical centers, which could enable the intensive light emission and therefore make them be promising materials for devices such as solar cells with high-efficiency, low-cost and light-emitting devices for those indirect band gap semiconductors of the IV group semiconductors[1-3] and halide perovskites [4-6]. Ion implantation has been demonstrated to be an effective way to bring in optical centers in silicon, which is an optically nonactivated materials but the footstone of the whole microelectronics, and are promising to promote the silicon to be the optimal candidate for realizing the great "optoelectronic and microelectronic integration" engineering.

Although the optical defects can be effectively formed in the Si film by Si^+ ion implantation and annealing processes on the top layer of the SOI substrate, the light emitting efficiency still can't meet the level of chip integration application[7, 8]. The integration of optical quantum amplification structures on the luminescent Si based materials, which is believed to be one of the most effective means, has attracted extensive attention in recent years to enhance the luminescence performance of the defect silicon. Periodical metal or semiconductor nanostructure array with certain dielectric constants was generally used to fabricate the photonic crystals, which can amply the light emission of solid matter.

Since the introduction of such optical defect mode requires the nano-level photolithographic process with the characteristic of sophisticated, complicated, and relatively high-cost, meanwhile the obtained photonic crystal exhibits a gain effect merely at a relatively small area within the micro-level range, the large-scale application of the silicon-based light-emitting materials photonic crystals with the defect mode is seriously limited.

Plasma enhanced luminescence on metal surfaces is also one of the current research hotspots. The radiation efficiency [9] of the luminous body was effected by the density of photon states according to calculations by Gontijo [10] et al. When the electromagnetic waves radiated [11] by the electronic transitions match the wavelength of the plasma resonance, the probability of excitons radiative transitions will be increased by 55 times. In addition, the luminous efficiency of the luminous body is given by the following formula:

$$\eta_{\text{inside}} = r_r/\left(r_r + r_n\right), \tag{1}$$

where, r_r is the radiative transition probability and r_n is the non-radiative transition probability. The luminous efficiency of the sample[12] is

$$\mathrm{Y} = \left|L\left(\omega_{\text{ex}}\right)\right|^2 Z\left(\omega_{\text{em}}\right), \tag{2}$$

where, $L\left(\omega_{\text{ex}}\right)$ term represents the local electric field intensity, and the $Z\left(\omega_{\text{em}}\right)$ one represents the energy distribution of the metal nanoparticles for radiative and non-radiative transitions.

The dynamic state of electromagnetic waves in media with different dielectric constants can be obtained by solving the Maxwell's equations. The principle of finite-difference time-domain method (FDTD) is solving Maxwell's equations by replacing the differential with difference between space and time, and constructing the Yee cell to mesh the space. Therefore, the FDTD simulation is believed to be an effective mean to acquire the parameters of photonic crystal, which could meet the expected experiment result.

In this work, FDTD was used to theoretically strengthen gains of luminous efficiency by simulating the structure and optimizing the parameters of photonic crystal in advance. Thus, the size of PS beads can be etched to the designed size by the ICP process, and a plasma enhanced luminescence SOI material [13, 14] with a photonic crystal structure can be acquired by depositing Au film on the periodically arranged spheres via the vacuum coating machine.

1 FDTD simulation

The PS spheres is arrayed in close-packed hexagonal pattern with the diameter of 500 nm. Generally, the ultimate penetration depth in the metal is between 10 nm and 100 nm, and the Si wafer size is set to 3.4 μm × ($\sqrt{3}$/2) 3.4 μm. The Si layer was set to 100 nm, and the number of beads was set to 6 × 6. The default dielectric constant of software is 2.56. The Perfect Metal Absorption Layer (PMAL) acts as the absorption layer and the number of absorption layers is set to 32.

Since the space is divided into grids to solve Maxwell's equations by the time domain difference method, the grid completely fills all the areas in the middle of the PML layer. Considering the simulated wavelength range is 700 nm-960 nm, the grid is set to 70 nm × 70nm. By taking the calculation speed and accuracy into account, a relatively small area is selected to place a new 1 nm × 1 nm × 1 nm grid, as the light source.

Purcell factor, in direct proportional to the enhancement factor, is used to illustrate the luminous intensity gain performance. Moreover, the Purcell factor is as follow:

$$F_{\text{p}} = \frac{3}{4\pi^2}\left(\frac{\lambda_c}{n}\right)^3\left(\frac{Q}{V}\right), \tag{3}$$

where, (λ_c/n) is the wavelength of the substance, Q and V are the quality factor and mode volume, respectively.

Mode volume V is mainly related to electric field distribution and dielectric constant.

2 Experiments

Since both Au nanospheres and nano-islands structures owned gain effects for the waveband beyond 700 nm, the luminescence of Si nanocrystals was enhanced by the plasma resonance of the Au film in this work. Since the plasma was mostly distributed on the metal surface, nanophotonic crystals array of Au film was designed to enhance luminescence, with the thickness and the hole diameter of Au film being 200 nm and 480 nm, respectively.

Figure 1 shows the specific experimental process as follows. First, samples were cleaned with the Shiraki method [15], and the cleaned samples were self-assembled with a layer of 500 nm diameter PS beads with the LB method. Second, etch the PS beads for 240 s with ICP. After the pellets were etched, PS beads were placed in a drying oven at 155 °C for 3 minutes, which were melted and softened to form pillars. The vacuum coating machine was utilized to vapor deposit the Au film of 200 nm thick. Finally, samples were annealed at 160 °C for 5 minutes, and the pellet was washed away in a tetrahydrofuran solution.

Figure 2 (a) and (b) show a sharp contrast of the simulated electric field intensity. The electric field intensity at the position of the nanopore is large, however, it is almost zero at the area covered by the Au film, which means that it is difficult for the light source to penetrate the Au film.

Figure 2 (c) shows the SEM characterization of the prepared sample, the holes and holes have been linked to each other. It is related to the preparation of the sample. Since the thickness of the Au film is 200 nm. Therefore, it is difficult to dissolve the PS beads only in the tetrahydrofuran solution completely. After annealing at 160 ℃ for 5 minutes, the PS beads will melt which will cause the holes of the Au film to be larger than the diameter of the PS spheres (220nm) in this process.

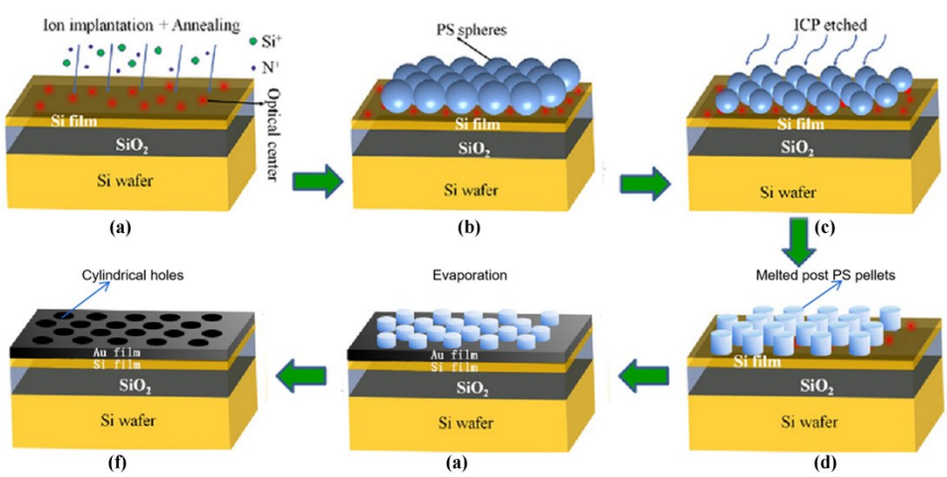

Fig. 1 Preparation process of Au film photonic crystal array.
图1金膜光子晶体阵列制备流程

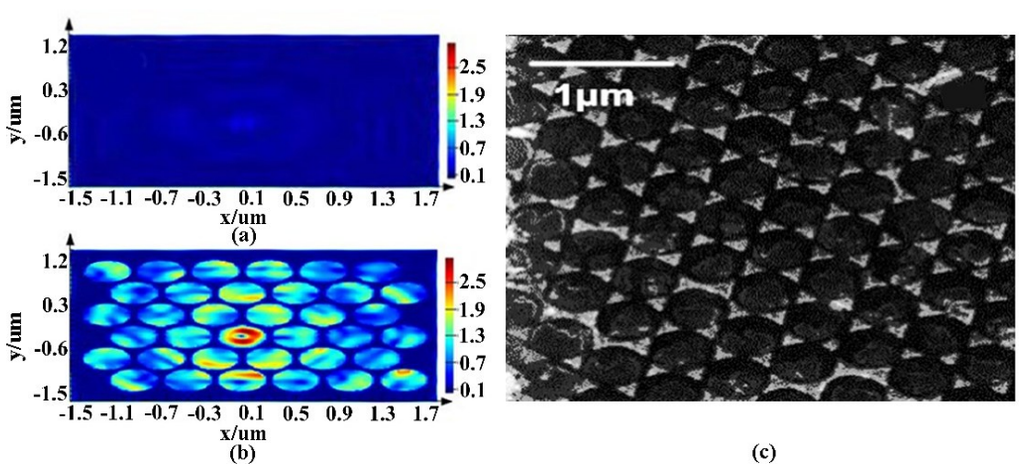

Fig. 2 (a) Simulation of electric field strength of Au film without photonic crystal structure (b) Simulation of electric field strength of Au film with photonic crystal structure (c) SEM characterization of Au film photonic crystal structure sample.
图2(a)不具有光子晶体结构的Au膜的电场强度的模拟(b)具有光子晶体结构的Au膜的电场强度的模拟(c)Au膜光子晶体结构样品的SEM表征。

3 Results and discussion

Figure 3 shows that the nanodisk photonic crystals structure has an effective enhancement on the PL intensity from the defect in SOI. In fact, the intensities of the two broadening PL peaks from the photonic crystals at the 760-820 nm and 830nm-960 nm band have been enhanced by 24 and 126 times in compared with the original PL ones, respectively. N^+ dose of 1×10^{14} cm^{-2} and Si^+ implantation dose of 5×10^{14} cm^{-2} were implanted in samples.

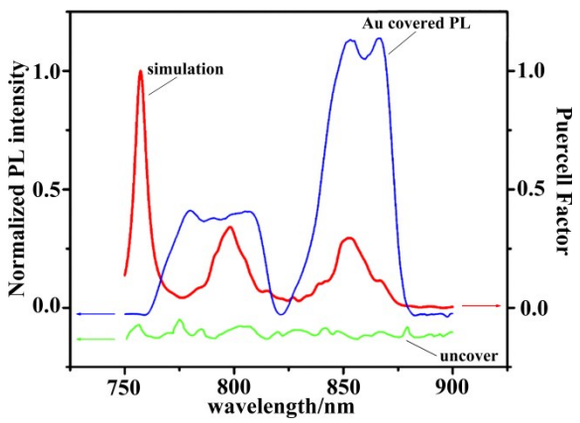

Fig. 3 PL spectra and Puercell factor of Si^+/Ni^+ ion co-implanted SOI nanodisk Au film sample and the uncovered sample as well as the simulated sample.
图3 Si^+/Ni^+离子共注入的SOI纳米盘金膜样品和未覆盖样品以及模拟样品的PL光谱和Puercell因子。

As shown in Figure 3, the two PL wave packs at 760~820 nm and 830~960 nm can basically consistent with the simulation results. There is a certain shift between the simulation results and the experimental results. This may be related to the introduction of defect modes in the photon forbidden band, and the energy level of the mode will greatly enhance the luminescence at that frequency. The enhancement of wave packets at 760~820 nm and 830-960nm is caused by the direct recombination emission of exciton from small and large nanocrystalline silicon crystals under the quantum confinement effect, respectively. Purcell factor plays a role of amplifying intrinsic luminescence. Nano-silicon crystals of different sizes are superimposed and formed Broad band. In addition, plasma photonic crystals have two enhanced luminescence mechanisms, both photonic crystal resonance and surface plasma resonance. The combination of these two effects leads to a frequency shift of the luminescence peak position, which also makes the actual PL spectrum of the sample and the simulated Purcell factor have a mismatch in some areas. The Purcell effect is mainly reflected in the enhancement of the spontaneous emission rate of the charge of the Au film photonic crystal of the periodic array relative to the unstructured charge, which also supports the enhancement of the photoluminescence effect. In addition, the enhancement of the normalized intensity of the PL wave packet at 760~820 nm by the photonic crystal is about 24 times, and the enhancement of the PL wave packet at 830-960nm is about 126 times, and the overall luminous peak intensity of the Au film sample is greater than that of the uncovered sample, which means that the nanodisk Au film array can effectively enhance the photoluminescence of Si^+/Ni^+ ions co-implanted with SOI.

Figure 4 shows the photon band gap diagram of the simulated the Au nanodisk-array photonic crystals. When the emission frequency of the material is within 3.6×10^{14}-3.7×10^{14} Hz, which is the photonic forbidden band, the normalized luminous intensity given by the simulation in Figure 3 is particularly low at 810 nm-830 nm (3.6×10^{14}-3.7×10^{14} Hz), which is also consistent with the luminescence of the Au film sample. Then Figure 4 shows a bottom U-shaped "photon level" appeared at the bottom of the forbidden band, which indicates that the light at 857 nm can be enhanced mostly, so there is a luminescence enhancement at 857 nm section. Compared with the simulation results, it has been substantially enhanced. This may be caused by the deformation of the dislocation strain region in the sample preparation process, which leads to the introduction of a defect "energy level" at 857 nm, which substantially enhances the spontaneity of the sample, similar to the photonic crystal with a defect mode.

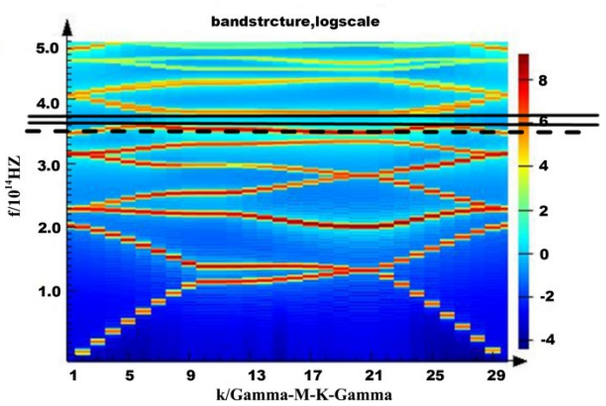

Fig. 4 The photonic band gap of the sample with the Au nanodisk-array photonic crystals which simulated by the FDTD software. The 3.6×10^{14}-3.7×10^{14} Hz (810~830 nm) range corresponding to the solid black line is the photonic forbidden band, and the black dotted line corresponds to the luminous peak at 3.5×10^{14} Hz (857nm).
图4带有FDTD软件模拟的Au纳米盘阵列光子晶体的样品的光子带隙。对应于实心黑色线的3.6×10^{14}~3.7×10^{14} Hz(810~830 nm)范围是光子禁带,黑色虚线对应于3.5×10^{14} Hz(857 nm)的发光峰。

4 Conclusion

A photoluminescence enhancement of SOI by Si^+/Ni^+ ions co-implantation process is introduced in this paper. The FDTD software was used to simulate the Au nanodisk-array photonic crystals, and the corresponding structural parameters and gain effects were obtained. In this work, film thickness and aperture of Au nanodisk-array photonic crystals holes is 200 nm and 480 nm, respectively. Subsequently, the SOI substrate with the

photonic crystal structure is prepared by PS balls and the metal coating. The experimental and simulated results show that the Au nanodisk-array photonic crystals not only have a substantial enhancement effect on the light on the horizontal plane and but also resonate with the plasma on the hole wall in the direction of propagation to effectively enhance the luminescence. In addition, the normalized intensity of the photonic crystal to the PL wave packets of 760~820 nm and 830~960 nm are increased by 24 times and 126 times, respectively. It is caused by the structurally stable defect emission center and the direct recombination emission of nano-silicon crystal exciton under the quantum confinement effect, respectively. In general, this work provides a simple and easy-to-use method for the preparation of effective luminescence-enhanced films that can be effective to sample with larger areas, and it can be approximately fitted with theoretical calculations, and it is beneficial to manufacture silicon-based light-emitting devices.

References

[1] Ouyang L, Wang C, Feng X, *et al*. Light emitting properties of Si+ self-ion implanted silicon-on-insulator from visible to infrared band [J]. *Optics Express*, 2018, **26**(12): 15899-15907.

[2] OuYang L, Wang C, Zhou M, *et al*. Light emitting from the self-interstitial clusters buried in the Si+ self-ion implanted Si films [J]. *Micro & Nano Letters*, 2017, **12**(4): 205-208.

[3] Wang C, Yang Y, Yang R-D, *et al*. Study on the defect-related emissions in the light self-ion-implanted Si films by a silicon-on-insulator structure [J]. *Chinese Physics B*, 2011, **20**(2): 026802.

[4] Qin Z, Dai S, Hadjiev V G, *et al*. Revealing the Origin of Luminescence Center in 0D Cs_4PbBr_6 Perovskite [J]. *Chemistry of Materials*, 2019, **31**(21): 9098-9104.

[5] Wang C, Wang Y, Su X, *et al*. Extrinsic Green Photoluminescence from the Edges of 2D Cesium Lead Halides [J]. 2019, **31**(33): 1902492.

[6] Qin Z, Dai S, Gajjela C C, *et al*. Spontaneous Formation of 2D/3D Heterostructures on the Edges of 2D Ruddlesden - Popper Hybrid Perovskite Crystals [J]. *Chemistry of Materials*, 2020, **32**(12): 5009-5015.

[7] Wang C, Chen D, Huang S, *et al*. Optical properties of D and S defects induced by Si+/Ni+ ions co-implanting into Si films on insulator [J]. *Nanotechnology*, 2020, **31**(24): 245704.

[8] He P, Wang C, Li C, *et al*. Optical properties of the low-energy Ge-implanted and annealed SiO2 films [J]. *Optical Materials*, 2015, **46**: 491-496.

[9] Wang C, Ke S, Hu W, *et al*. Review of Quantum Dot-in-a-Well Infrared Photodetectors and Prospect of New Structures [J]. *Journal of Nanoscience and Nanotechnology*, 2016, **16**(8): 8046-8054.

[10] Gontijo I, Boroditsky M, Yablonovitch E, *et al*. Coupling of InGaN quantum-well photoluminescence to silver surface plasmons [J]. *Physical Review B*, 1999, **60**(16): 11564-11567.

[11] Liu C, Wang C, Chen X, *et al*. Analysis of direct current performance on N-polar GaN-based high-electron-mobility transistors for next-generation optoelectronic devices [J]. *Optical and Quantum Electronics*, 2015, **47**(8): 2479-2488.

[12] Lakowicz J R. Radiative decay engineering: Biophysical and biomedical applications [J]. *Analytical Biochemistry*, 2001, **298**(1): 1-24.

[13] Wang C, Ke S Y, Yang J, *et al*. Electronic properties of single Ge/Si quantum dot grown by ion beam sputtering deposition [J]. *Nanotechnology*, 2015, **26**(10): 105201.

[14] Ke S, Ye S, Yang J, *et al*. Morphological evolution of self-assembled SiGe islands based on a mixed-phase pre-SiGe island layer grown by ion beam sputtering deposition [J]. *Applied Surface Science*, 2015, **328**: 387-394.

[15] Ke S Y, Yang J, Qiu F, *et al*. Secondary growth mechanism of SiGe islands deposited on a mixed-phase microcrystalline Si by ion beam co-sputtering [J]. *Nanotechnology*, 2015, **26**(44):445602.